JOURNAL OF SPACECRAFT AND ROCKETS
Vol. 42, No. 1, January–February 2005

Ionospheric Instability Observed in Low Earth Orbit Using Global Positioning System

Leonard Kramer* and John L. Goodman†
United Space Alliance, L.L.C. Houston, Texas 77058

The global positioning system (GPS) receiver used for navigation on the space shuttle exhibits range rate noise that appears to result from scintillation of the satellite signals by irregularities in ionospheric plasma. The noise events cluster in geographic regions previously identified as being susceptible to instability and disturbed ionospheric conditions. These mechanisms are reviewed in the context of the GPS observations. Range-rate data continuously monitored during the free-orbit phase of several space shuttle missions reveals global-scale distribution of ionospheric irregularities. Equatorial events cluster $\pm 20^\circ$ about the magnetic equator and polar events exhibit hemispheric asymmetry suggesting influence of an off-axis geomagnetic polar oval system. The diurnal, seasonal, and geographic distribution is compared to previous work concerning equatorial spread F, Appleton anomaly, and polar oval. The observations provide a succinct demonstration of the utility of space-based ionospheric monitoring using GPS. The susceptibility of GPS receivers to scintillation represents an unanticipated technical risk not factored into the selection of receivers for the U.S. space program.

Nomenclature

$\boldsymbol{A}_\perp$	=	perpendicular component of vector $\boldsymbol{A}$
$\boldsymbol{A}_\parallel$	=	parallel component of vector $\boldsymbol{A}$
c	=	speed of light (const)
E	=	electric field of electromagnetic radiation
S_n	=	arbitrary path in space between transmitter and receiver
V	=	spacecraft velocity
α	=	angle from spacecraft velocity vector to line of sight to global positioning system satellite
β	=	angle between spacecraft velocity vector and local geomagnetic field
ϵ	=	permittivity of material media (e.g., ionospheric plasma)
ϵ_0	=	permittivity of free space, a physical constant
Φ	=	phase envelope of an interference distribution
ϕ	=	phase of electromagnetic radiation resulting from propagation in space
ω	=	circular frequency of radiation, radians per unit time
ω_P	=	plasma frequency of radiation, radians per unit time

Introduction

IN EVALUATING the global positioning system (GPS) receiver intended for eventual replacement of onboard tactical area navigation (TACAN) systems currently in use for entry and landing of the U.S. Space Shuttle, we have incidentally observed rather unambiguous evidence of ionospheric scintillation in the receiver velocity measurements.[1] The receiver, known as a miniaturized airborne GPS receiver/space (MAGR/S) is a five-channel, dual-frequency (L1, L2) receiver "keyed" to receive military secure Y code in addition to less-precise C/A-coded GPS signals. The receiver has been specially adapted by the manufacturer, Rockwell-Collins, for spaceflight use.[2] In the early phases of receiver evaluation, periods of noisy velocity in the output state from the GPS receiver were observed by ground controllers. The phenomenon, shown in Fig. 1, was seen in many consecutive orbits and would persist for 10 to up to 20 min. Subsequent analysis indicates that this noise is related to delta-phase, range-rate measurements which usually cluster around the magnetic equator. The noise is a source of concern to the manned space effort because it exceeds nominal system requirement thresholds.

Since at least the early 1950s, ionospheric irregularities have been known to contribute to interruptions in radio communication. This disturbance is known as scintillation and the processes creating it show global-scale effects. Many studies document observational and theoretical bases for scintillation of radio frequency radiation. The most important of these involve instability processes connected with neutral thermospheric atmosphere circulation and the geomagnetic field in equatorial regions and particle precipitation related to aurora in the polar cap latitudes. Aarons[3] has articulated theories related to the geographic and seasonal occurrence of equatorial scintillation. More recently, studies have further documented the seasonal and space weather forcing of the disturbances.[4] Kelley gives an extensive discussion on the geophysical causes and consequences of ionospheric irregularities.[5] Efforts have been undertaken to create GPS-based ionosphere monitoring systems based on ground-based systems.[6,7]

The GPS system, utilizing a dual-L-band frequency (1.57542 and 1.2276 GHz) signal, is subject to scintillation and can be used to monitor the global nature of ionospheric processes contributing to scintillation and perhaps better understand these processes. We assert that the noise seen in the velocity is a result of ionospheric scintillation of the range-rate measurements. In this work we develop techniques to diagnose scintillation from range rate measurements. We present geographic and, to the extent possible, the seasonal and solar-hour-angle dependence of our events. We also describe a theoretical basis for spacecraft velocity augmentation of the effect and observational evidence supporting it.

We would like to advance the idea that satellite-borne GPS receivers in low Earth orbit (LEO) can contribute to the global understanding of occurrence and geophysical causes of ionospheric irregularities. Also, scintillation of GPS is one of the several factors that contribute to the technical risk of using off-the-shelf terrestrial-based receivers for high-performance orbital applications.[8]

Data

As part of GPS receiver evaluation, auxiliary instrumentation port data are regularly collected during orbital phases of shuttle flights. These data comprise internal software parameters, pseudorange and delta-phase range rate information in four simultaneously tracked

Presented as Paper 2001-4653 at Space 2001...The Odyssey Continues, Albuquerque, NM, 28–30 August 2001; received 19 June 2003; revision received 24 October 2003; accepted for publication 16 January 2004.

*Engineering Staff, Navigation, 600 Gemini Avenue, USH-485L.
†Engineering Staff, Navigation, 600 Gemini Avenue, USH-485L. Member AIAA.

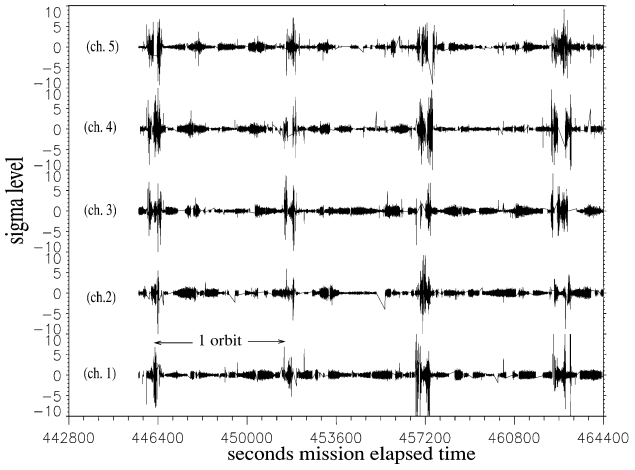

Fig. 1 Evidence of scintillation of MAGR/S on STS 99 orbits. The range-rate residuals are normalized to the projection of receiver state error in the range-rate space.

GPS satellites, and an additional peripheral channel that monitors satellite selection and the dual-frequency correction needed to compensate for ionospheric delay. The total electron count (TEC) is not directly reported by the receiver; however, pseudoranges are available and could be used to compute TEC directly if needed for any follow-up investigation. The MAGR/S receiver software computes a state (position and velocity) using a blended-solution Kalman filter employing process noise intentionally tuned to suboptimum levels. The practice makes the receiver generically robust because uncertainty in the filter state grows quickly when measurements are absent and, thus, current measurements are always heavily weighted in the solution. It is fair to say that, in a sense, the receiver is not using a Kalman filter, but rather that it delivers a blended deterministic solution. The downside of the practice is that the receiver will not effectively incorporate information from known orbit physics. Thus, accuracy is always limited by the intrinsic accuracy of the immediate measurements. A good Kalman filter, employing high-fidelity physics models, will permit accuracy to improve significantly as measurements are incorporated into the state. In practical terms, the states from the MAGR/S are generally unsuitable for precise on-orbit navigation or rendezvous. This suboptimal nature of the receiver is a consequence of a deliberate decision not to exceed the relatively coarse requirements of the existing TACAN system for entry and landing.

Range Rate Measurements

The data in this investigation comprise 0.2-s period, phase-change observables constituting range-rate measurements. Normally the phase rate of the L1 frequency is measured. However, the receiver will revert to L2 during off-nominal conditions if available. Both pseudorange and range rate are incorporated into the receiver's state estimate. Inertial information is contributed in the form of aiding data from the shuttle onboard solution and a barometric reading is used to augment altitude on entry and landing. As part of the usual state processing in the GPS internal filter, residuals are formed that represent a difference between the state's projection of range rate and the actual range-rate measurement. These residuals are then normalized to the projection of the Kalman filter covariance in the range-rate space. Figure 1 presents a time series of some of these observations from a shuttle mission in February of 2000. These signatures form the principle evidence of scintillation that we have seen.

For independent measurements with Gaussian distributed instrumental error, the normalized observations should theoretically correspond to a standard normal distribution with the caveat that the filter state has converged and is tuned appropriately. Therefore the noise seen in Fig. 1, with level exceeding 2 or 3, seems to represent profoundly corrupt measurements in the sense that they are significantly off nominal with respect to the representative distributions of these data. Despite outlier detection logic in the receiver's Kalman filter, they are incorporated into the filter state and tend to damage the receiver solution. As we mention in our conclusions, the shuttle program has been concerned about the affect of these noise events on operations.

We do not typically see pseudorange noise at the same time as the range-rate noise as shown in the Fig. 1 example. For some events, the internal filter state is sufficiently perturbed by bad range rate to cause errors to appear in the pseudorange residuals. This is almost certainly a result of the filter state being in error rather than the ranges exhibiting noise. The receiver state's velocity becomes corrupted when the noise appears in multiple channels. Because the pseudorange is observed by mixing the receiver signal with a long-wavelength random code, we speculate that the correlation signal strength of these pseudorange measurements will be reduced but the long wavelength of the code appears to protect the pseudorange compared to phase rates. We have not yet examined this in detail.

In our evaluation of the MAGR/S we have documented other anomalies contributing to noisy ranges related to GPS receiver operation and software anomalies. Sources of noisy GPS velocity include 1) suboptimal intermediate satellite geometry due to "one-at-a-time" changes in selected satellites, where changes have been delayed by software anomalies or poor visibility with respect to antenna gain pattern; 2) suboptimal satellite geometry and less than four satellite tracking caused by signal obscuration while docked to Mir, the International Space Station, or the Hubble Space Telescope; 3) occasional receiver restarts due to internally detected software anomalies; and 4) switching of satellites tracked for navigation measurements, which is due to the Kalman filter implementation.

Noisy GPS velocity that results from the aforementioned sources has a different signature and often a higher magnitude than that caused by the ionospheric scintillation seen in Fig. 1. Furthermore, times of suboptimal geometry and receiver resets are known and can be compared against noisy velocity periods. Space shuttle flights of the MAGR/S, beginning in September 1996, have led to numerous receiver software changes. As software corrections were applied, the number of nonscintillation noisy velocity incidents decreased.

Scanner Code

Our approach to the data in the present work is to identify noisy periods based on the normalized delta ranges. We have identified scintillation on numerous flights. In this work we have selected four flights to study in detail. Referring to the normalized units in Fig. 1 as "sigma level," we have written a scanner program that selects events based on that sigma level. The characteristics of the selection algorithm are as follows:

1) Sigma level exceeds 2 for 2 s (2 measurement cycles) or more.
2) Measurement must be 3 s after a set of satellites are selected.
3) Receiver has a good lock on the satellite (FOM = 1).

We selected a sigma-level threshold of 2 based on accumulated histograms of normalized range-rate observations. These indicate that greater than two sigma measurements are profound outliers when compared to the background distribution. Criterion 2 reflects awareness of a known deficiency of the system in that the receiver state does not solve for range biases. When a set of four satellites are assigned to hardware channels, the existing state covariance is not adjusted to reflect increased uncertainty in a new state. As a result, anomalous sigma levels appear in the measurements. Excluding events for 3 s permits influence of the satellite set switch to be absorbed into the state. The third criterion is to simply mask against the internal figure of merit (FOM) calculated by the receiver. Selecting events with good FOM reduces effects of poor tracking due to blockage and software deficiency.

The event selection list does not exhaust all alternate sources for false positive detection of scintillation. For example, there is statistical clustering of noisy events in the range rate immediately before a set of satellites is switched. This may be the result of some sensitivity to weak signal associated with factors contributing to satellite switching logic. The issue is still under study.

Events meeting the scanner criterion are further processed to evaluate latitude and longitude, solar hour angle, and geomagnetic field at the event position. The lines of sight to all four satellites are

computed and satellite attitude angles between the spacecraft velocity vector, the geomagnetic field, and local horizontal are also computed. The latitude and longitude of the event are at the shuttle position, not any arbitrary subionospheric "pierce point" as has been done in some of the literature.

Our scanner algorithm is our attempt to automate the discrimination between the scintillation signature and the noise signatures from the listed deficiencies. It is unlikely that we have completely succeeded in this regard but we proceed as a best effort, balancing simplicity with thoroughness. We could, for example, refine our scanner algorithm with an elaborate cascade of tests to exclude more of what we believe to be nongeophysical signatures, but we are concerned that this detailed approach would introduce too much subjectivity in the scanner.

Geographic Distribution

The shuttle orbits the Earth approximately every 90 min and so the LEO platform samples all geographic longitudes in a few days. Compared to ground-based observations, little variation in solar hour angle is afforded. This is because the solar hour angle at a particular latitude does not vary much during the orbit and only as a result of the orbit motion of the Earth around the sun during the mission and the precession of the spacecraft orbit as a result of the Earth's oblateness. Evidently shuttle-based observations permit a wide geographic sampling with comparatively little ability to observe solar-hour-angle variation (at a given latitude) in the geophysical process.

Figure 2 presents the geographic clustering for four missions. Geomagnetic dip angles at ± 15 and 45 deg are superimposed on the plots as well as the geomagnetic equator. In Fig. 2a, we see the latitude–longitude distributions for STS 88, which was flown at an inclination of 51.6 deg on 4–15 December 1998. The northern and southern limits are dictated by the limited inclination of the orbit. There are a large number of false positive scintillation signatures in Fig. 2a which manifest as isolated events occurring throughout the plot. We believe that the significant software changes mentioned previously, which are related to errors identified during evaluation of the receiver, are responsible for these false positive events. Many of the software issues were corrected subsequent to this flight. Nevertheless, in Fig. 2a we see clustering of linear trains of events along the inclined orbital tract occurring over equatorial regions of South America. These are seen on consecutive orbits, stretching eastward across the equatorial Atlantic Ocean. Events taper off over western to central sub-Saharan Africa. Other linear strings of events occur over the Indian Ocean, southwest of India and over Sumatra, and eastward over central regions of Indonesia.

In addition, there is a hint of clustering of events near the most poleward extent of the spacecraft's orbit, suggesting that we are intercepting scintillated signals through auroral zones. As a result of the large number of false positive events on STS 88 (Fig. 2a), the conclusion that we are seeing auroral scintillation is tentative. We would also caution that latitude sampling of any purely random process is biased toward higher latitudes by the approximately sinusoidal variation of latitude with respect to longitude as the spacecraft orbits. We can say that the appearance of individual time series for STS 88 that we examine for events occurring south of Australia in particular is consistent with the morphology of scintillation signatures seen in the equatorial regions. In other words, we have confidence that we are seeing some auroral zone scintillation on STS 88 in Fig. 2a.

In Fig. 2b we see the geographic distribution of scintillation events from STS 96 flown from 27 May to 6 June 1999 and inclined at 51.6 deg. The results from current mission contrast to that in STS 88 seen in Fig. 2a. We believe that the number of false positive signatures is greatly reduced as a result of the significant software changes mentioned previously. But in addition, the number, degree,

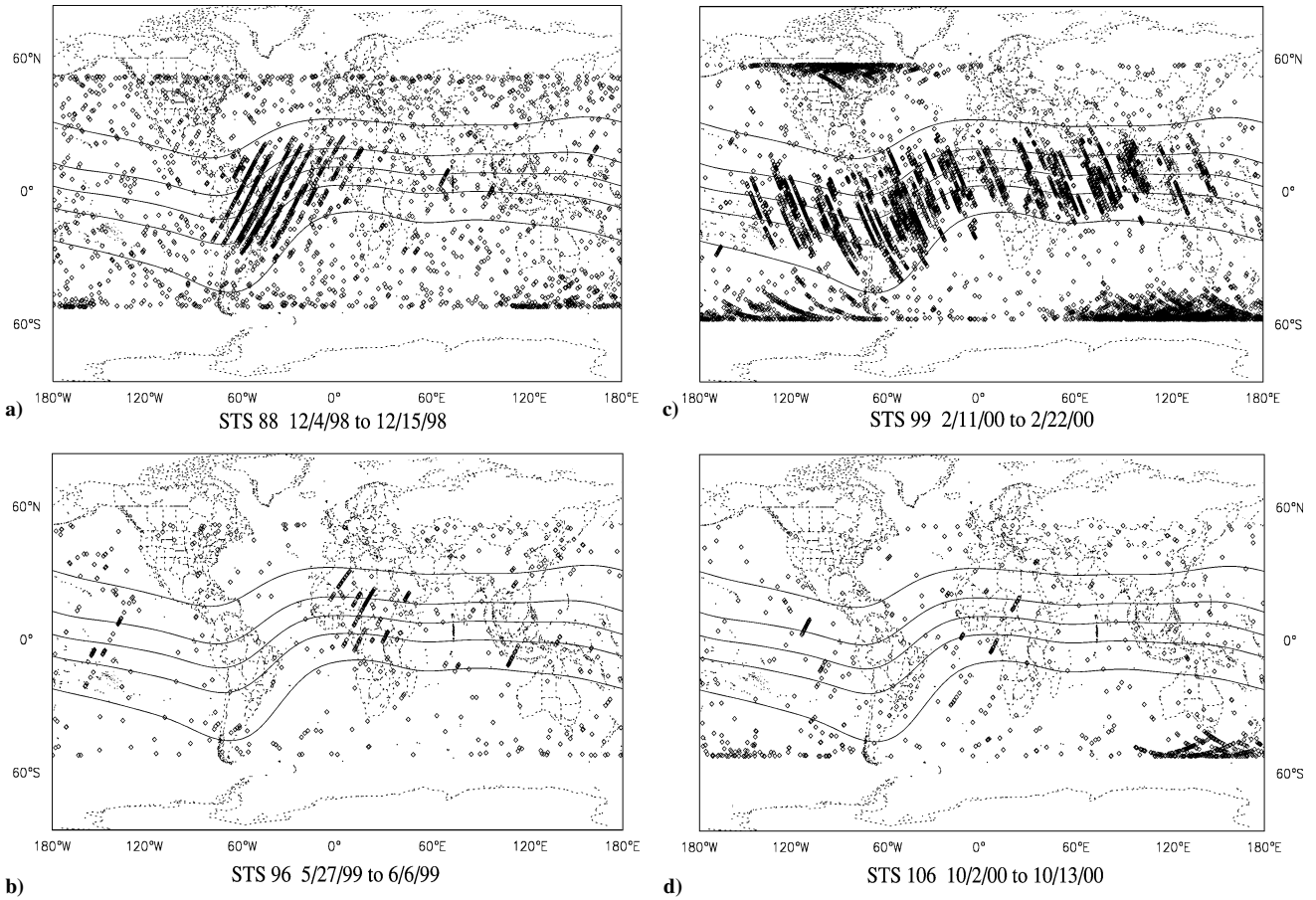

Fig. 2 Geographic distribution of noise events seen in GPS receiver range rate for space shuttle. Geomagnetic equator and dip-angle contours shown at ± 15 and 45 deg. A wide range of activity and clustering of events near the geomagnetic equator and in polar regions is noted. The record for STS 88 seen in panel a may have many false positive events resulting from now-corrected software issues.

and extent of what we identify as scintillation is reduced as well. The primary contributions are from linear tracks of events along ascending portions of orbits occurring over the east-central Pacific and a group of events again occurring over central and northern Africa. Indonesia also appears to be favored with a significant event during this period. It is interesting that the event over the east-central Pacific Ocean is isolated yet extends from the dip-angle contour at 45 deg in the Southern Hemisphere all of the way to the conjugate dip latitude in the Northern Hemisphere. That event is accompanied by one other orbital track with greatly reduced extent.

The geographical extent of scintillation observed on STS 99, which flew 11–22 February, is shown in Fig. 2c. STS 99 had a 57-deg inclination and reached higher latitudes than the other studied missions. These results are in striking contrast to those seen for STS 96 and STS 88. Here, we assert, is broad extent scintillation in the equatorial regions roughly bracketed by the dip-angle contours at 45 deg in both Northern and Southern Hemispheres. The events are seen on very many consecutive orbits stretching from the east-central Pacific across South America, continuing uninterrupted across the equatorial Atlantic, with some lessening of incidence across Africa but continuing over the Indian, Ocean, India, southeast Asia, and the western Pacific. Events are absent from the central Pacific region. There is also clear evidence of polar events distributed geographically that are somewhat consistent with known locations of the auroral zones–polar oval systems for the geographic coverage afforded by the spacecraft orbit. These are over east-central Canada and the north-central United States.[9,10] There is an absence of events with similar character over other Northern Hemisphere polar regions. In the Southern Hemisphere, the polar events are distributed with the greatest density south of Australia and the Indian Ocean. Significant activity is also present over the extreme south-central Pacific. It is significant that the equatorial zone very nearly merges with the polar events south of continental South America.

Finally, Fig. 2d presents latitude/longitude distribution of scintillation events for STS 106, which flew 2–13 October 2000 and had an inclination of 51.6 deg. Here, scintillation is very much reduced from that for STS 99. Equatorial events for STS 106 are seen in the eastern Pacific and once again over Africa. Southern polar events are very much in evidence but with no apparent significant activity in the Northern Hemisphere for this time.

The observations are consistent with previously identified regions where scintillation is believed to occur and the variation from mission to mission is consistent with seasonal variability published previously.[3,4] The STS 99 case in Fig. 2c exhibits scintillation measurements that are broader in global extent than any presented in the literature of which we are aware.

Instabilities

As we mentioned in our introduction, two geographic regions are of interest in contributing to disturbances in ionospheric plasma. The more important of these is the equatorial regions within about 20 to 30° latitude of the geomagnetic dip equator roughly corresponding to dip angles of ±45 deg. Anderson[11] and others describe the dynamics of the equatorial zone, which involves complex aeronomy featuring influence from the geomagnetic field, neutral atmosphere, ionosphere, solar radiation, and planetary rotation.

Because the ionospheric plasma is magnetized as a result of Earth's field, the charged electrons and ions are constrained to move in quasi-circular "orbits" around field lines when collisions are infrequent but are relatively unconstrained in the direction parallel to the magnetic field. The field is not dipolar but can be accurately modeled as we have shown in Fig. 2. In equatorial regions, the field is horizontal and assumes crescent-shaped arcs that are more or less meridionally oriented. As we approach a pole along a field line, the field assumes a vertical aspect or dip angle. In Fig. 2, we illustrate dip-angle contours from a standard model corresponding to the magnetic equator (±15 and ±45 deg dip angle). The 45-deg dip angle provides a logical division between equatorial and high latitudes.

For many years it has been recognized that there exists an equatorial ionospheric disturbance known as spread F which occurs as a result of a magnetic field-gravitational Rayleigh–Taylor mode in the equatorial regions after sunset within about 15 to 25° of the magnetic equator. This instability is analogous to that which occurs when a layer of buoyant fluid rises though a heavier fluid. Kelley[5] and Aarons[3] highlight the essential physics and observations that we review here including the description of plumes of ionospheric density depletions seen in backscatter radar that rise as high as 1000 km.

We would also like to point out that, although we have broadly categorized equatorial events as occurring within ±45 deg dip angle of the geomagnetic equator, the equatorial events extend beyond this limit in the south-central Atlantic Ocean. These events are seen in Figs. 2a, 2c, and 2d. We think this is related to significantly weaker magnetic field at this location and is coincident with the well-known South Atlantic Anomaly. We postulate that the crescent-shaped meridionally oriented structures thought to comprise the events rise to higher altitudes and extend to wider latitudinal extent as a result of the weaker geomagnetic field which would permit greater crossfield motion of ions at these points.

Furthermore, the radiation hazard cited for astronaut safety in the South Atlantic Anomaly is entirely independent from processes associated with scintillation and we have no theoretical basis to assume that the high-energy particles entering the Earth's ionosphere in the region during geomagnetic storms directly cause scintillation of the GPS L-band signals. However, coincidental thermospheric heating and changes in neutral atmosphere circulation might, we speculate, introduce variability to the process that contributes to spread F.

Scintillation is also observed in the polar regions. Much of the same complexity attached to equatorial regions also applies to the polar ionosphere.[12] In addition, geomagnetic field lines in the high-latitude regions map to the magnetosphere and the interplanetary medium connecting with the solar wind and embedded magnetic field. As a result of the nonaxially symmetric contributions to the Earth's field and partly as a result of the attendant diurnal and space weather forcing, polar scintillation should not distribute symmetrically around the poles.

Variability from mission to mission is striking and might be explained by known seasonal and solar weather dependence of the factors that contribute to scintillation. The noise we are observing is globally extensive and consistent with equatorial incidence cited in previous work. Previously identified features at polar latitudes are also observed. Aarons[3] points out that the known selective factors that contribute to the global scale occurrence of scintillation are modulated by neutral wind and electric field changes, which are not well understood and which can theoretically either enhance or inhibit the development of the irregularities. Understanding of the seasonal forcing should improve in the coming years.

Solar Angle

The satellite-based technique does not permit exhaustive sampling of solar hour angle as was mentioned previously. Nevertheless, we can investigate solar-hour-angle occurrence for the few hours local time represented by each of the flights studied. Figure 3 shows the solar-hour-angle occurrence divided between equatorial and polar events. Polar events are separated from equatorial events by sorting according to magnetic dip angle and forming histograms by number of events that occurred in solar-hour-angle bins. From Fig. 2, for example, it is evident that polar events may be separated from equatorial events by a dip angle equal to 45 deg. The only exception are those events occurring in the South Atlantic that we mentioned previously and the false positive events that are most prominent for STS 88 in Fig. 2b. Figure 3, showing our solar-hour distributions, should not be interpreted as describing any significant composite diurnal variability. The differences in event occurrence seen between missions is certainly dominated by seasonal and space weather effects rather than a manifestation of diurnal variability.

The geophysical processes controlling equatorial spread F phenomena are associated with plasma instabilities occurring after dusk. In Fig. 3a we show solar-hour-angle distributions of equatorial scintillation events. The solar-hour-angle trace for STS 99 shows the largest number of events occurring primarily between 0100 and 0600 hrs but we emphasize that this was the only opportunity to

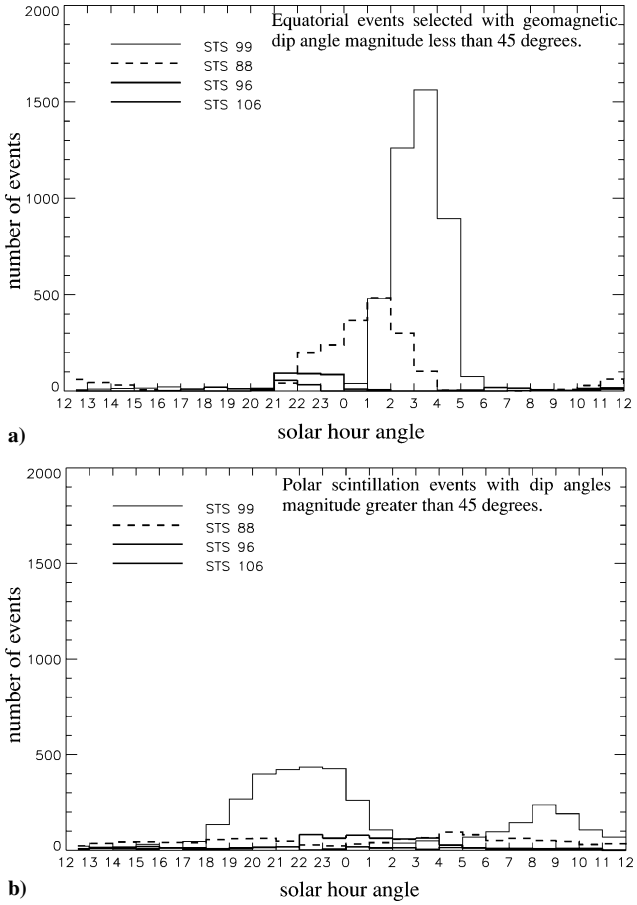

Fig. 3 Solar-hour-angle distributions of scintillation events divided between polar and equatorial regimes. Equatorial scintillation is a nightside phenomenon.

observe during nightside passes. A comparable period of time was available on the day side between about 1200 and 1800 hrs for STS 99, but we see no significant activity evident during the period. This shows that the equatorial process contributing to the scintillation may be prominent during the time between midnight and dawn and not just during the postsunset period, a point which has also been made in the literature.[13]

Similarly, the results for STS 88 show prominent equatorial activity between 2200 and 0400 hrs, which was the interval of time on the night side available for observation, whereas the opposite sides of these orbits on the day side show a small elevation in activity which we can attribute to the false positive phenomenon described earlier. The events for STS 96 and STS 106 also cluster in the nightside period.

The overall impression from Fig. 3a is that the equatorial scintillation we are observing is a nightside phenomenon. This is particularly established by the results from STS 99 and STS 88, where the majority of equatorial events are registered on the night side despite equal opportunity to observe on the conjugate dayside hour angles. We would add that sampling of orbits on the night side also explains the prominence of either ascending or descending orbit tracks seen in Fig. 2. For example, for STS 99 seen in Fig. 2c, the predominance of descending tracks from northwest to southeast in the equatorial zone is a result of scintillation selecting those portions of the orbit on the night side. Few ascending tracks were available on the night side.

The polar events do not have any particular diurnal clustering. The plot in Fig. 3b is dominated again by events sampled during STS 99, which is seen in the geographic latitude–longitude distribution of Fig. 2c to be extensive and unambiguously clustered at the poleward extremes of the orbit.

Interference Pattern

Scintillation might be thought to result from two sources. These are temporal variations in 1) total number of charge carriers in the plasma between transmitter and receiver and 2) the diffraction and refraction from and through irregularities in ionospheric plasma.

The TEC along the line of sight contributes to a first-order phase error or shift in phase of the signal. TEC is effectively measured by the dual-frequency receiver, and the corresponding range measurement compensation is expected to be very accurate based on the theoretical understanding of plasma. However, the compensation only corrects the range; the phase still changes as TEC changes and this will alias a range rate. From observations reduced to synoptic maps of TEC (for example, Fig. 8 of Ref. 6), we can estimate representative horizontal gradient in the phase delay and infer an order-of-magnitude estimate of the corresponding range-rate error from TEC variation. By our reading of the figure in Ref. 6, an upper limit on the horizontal gradient is 50 ns equivalent L1 range error over a 500-km horizontal path. At an orbit speed on the order of 10 km/s we would have a range-rate error from variation in TEC on the order of 1 ns/s, which amounts to 0.1 to 0.3 m/s range-rate error. This is a significant variation but occurs over a long period of time compared to the variations we observe, which have periods of a few to tens of seconds. Also, the receiver filter logic solves for clock bias rate, absorbing part of the range-rate error if it is persistent but slowly varying, and has a common component among all channels being tracked. Thus, the receiver will correctly adapt somewhat to short-term biases in range rate, at least to the extent that they are physically separable from a net velocity alias.

The second potential source of scintillation is the result of interference among multiple geometric paths between the satellite and the receiver. In electrodynamic theory, transmitted photons exhibit interference from multiple available paths. The received signal is contributed by the paths that exhibit the least first-order variation in phase from one another.[14] Conventional analytical and experimental results of optics are explained using this theory. Landau and Lifshitz draw these conclusions from their "eikonal equation" in their discussion about geometrical optics.[15] The least time principle, attributed to Fermat, and, the straight line propagation of light in a uniform medium are derived from it. In the ionosphere, as a result of the stochastic distribution of dispersive layers and inhomogeneities, these multiple paths are geometrically far apart compared to the wavelength and are apparently changing rapidly. The rapid change can be a result of both secular motion and motion of the receiver.

Historically, diffraction is classified by the size of the diffracting system relative to the distance from the receiver and source. Fresnel diffraction refers to interference effects that arise from a limited area of the diffracting system when the receiver is close to that system. Fraunhoffer diffraction refers to a far-field result that includes contributions from the entire diffracting system. Scintillation is sometimes categorized in terms of phase fading or amplitude fading. Except for the phase variations that result from changing TEC, theory causes us to view the physics of interference as contributing to both amplitude and rapid phase variation. The distinction between phase and amplitude fading must be significantly influenced by individual variability in how receivers process data. It has certainly been noticed that the degree of susceptibility to interference is highly receiver dependent.[10] It appears that the shuttle's MAGR/S is quite sensitive to phase noise, which explains the observations we see in Fig. 1.

Ground-based observations of scintillation would seem to be far field and formally outside of the Fresnel zone diffraction limit. This is because the distance from the interfering medium (hundreds of kilometers) is large compared to the dimension (tens to thousands of meters) of the diffracting inhomogeneities. The space shuttle orbits at altitudes that are essentially in the midst of altitudes where the diffraction is believed to originate. The shuttle environment is likely experiencing significant interference inside of the Fresnel zone.

Electrodynamics of Plasma

The structure of the planetary atmosphere can be studied from analysis of radiation transiting the medium. The received signal contains information from all areas of the ionosphere illuminated by the radiation from the transmitter. This principle is exploited

in many contributions to planetary atmosphere and ionosphere investigations. The recent work by Sokolovskiy and the references therein discuss the techniques for radioholographic inversion and radio occultation. As presented by Sokolovskiy these have been applied to the GPS/meteorological (GPS/MET) experiment and to the challenging minisatellite payload (CHAMP.)[16,17] The multiple-phase screen method featured in these papers essentially integrates the phase of the radiation through an atmospheric volume. Spacial inhomogeneities in the index of refraction caused by variable distribution of water vapor and temperature contribute to a modulation of the radiation wave front as it propagates through the volume. The same general mechanism applies to the ionosphere. Ionospheric profiles based on the Abel transform inversion technique have been applied to the ionosphere.[18] There appears to be a great deal of research activity in this area and we should expect more results in coming years.

In the space shuttle application, software logic masks satellite tracking below about 5 deg from local horizontal. Therefore, scintillation is singularly related to ionospheric disturbances. The primary contribution to index of refraction in the ionosphere may be derived from plasma theory. At the GPS L-band frequencies a high-frequency, cold-plasma limit applies and the only contribution to permittivity is

$$\varepsilon(\boldsymbol{x}, t) = \left\{1 - [\omega_P(\boldsymbol{x}, t)/\omega]^2\right\}\varepsilon_0 \tag{1}$$

The plasma frequency $\omega_P(\boldsymbol{x}, t)$, which appears in Eq. (1), represents a normal mode frequency associated with displacement of the electrons relative to the heavy positive charge carriers in the plasma (primarily O^+ in LEO). To derive this expression, the Maxwell equations and the equation of motion for the charged species are expressed in a fourier spacial wave number time frequency domain. Algebraic manipulation then permits a dispersion relation to be expressed that provides the analytical tool needed to understand how wavelength is related to the frequency and index of refraction in the media.

Equation (1) is a high-frequency limit to that general dispersion relationship which is appropriate because all the physical cutoffs and resonance such as electrons, ion gyro frequencies, plasma, and hybrid frequencies are orders of magnitude smaller than the GPS signal frequency. The relative simplicity of Eq. (1) reflects an advantage of high frequency for use in GPS. Readers are referred to a book by Swanson[19] which we think is a good treatment on the details of this analysis. An alternate approach is the Hartree–Foch equation exposed by Klobuchar,[20] which is a formulation that explicitly and appropriately neglects motion of ions but otherwise is identical. We would like to note especially that Eq. (1) contains no electron collision frequency or ohmic conductivity term and is positive real valued. This means that the frequency is high enough that the propagating mode exhibits no loss. Without an electron collision frequency term there is no theoretical basis to expect any decaying amplitude as there would be in a high loss medium like seawater, for example.

As the GPS signal transits the medium, the net effect is an accumulated phase shift over all possible paths between the transmitter and the receiver. For any geometric path between transmitter and receiver, the phase contribution to the total signal is computed according to

$$\delta\phi_{S_n} = \frac{\omega}{c\sqrt{\varepsilon_0}} \int_{S_n} \sqrt{\varepsilon(\boldsymbol{x}, t)}\, \mathrm{d}S \tag{2}$$

Equation (2) is really nothing more than a line integral off the component of wave number projected along the path S_n. This expresses the combined phase change along any arbitrary path which might even be tortuous and convoluted. The wave number is a function of the material property that is variable along the path.

Variational methods of calculus of might be used to determine a dominant path for mathematically tractable problems, but the physical principle is that all paths providing first-order invariant phase to the received signal will actually contribute to the received signal. All other paths will destructively interfere and cancel out. Both the electric and magnetic fields of the wave are modulated by the interference. This is why we would experience amplitude fading of signals. Conventional receivers respond to currents induced in the antenna by the electric field. The Fourier resolution in frequency of the radiation electric field becomes

$$\begin{aligned} E(\boldsymbol{x}, t) &= E_0 \sum_n e^{i(\delta\phi_{S_n} - \omega t)} \\ &= E_0 e^{-i\omega t} \sum_n e^{i\delta\phi_{S_n}} \\ &= E_0 e^{-i\omega t}\Phi(\boldsymbol{x}, t) \end{aligned} \tag{3}$$

where $E_0 e^{-i\omega t}$ is the electric field at the transmitter. The summation is taken over all available paths. Equation (3) represents a broad "sketch" of phase screen techniques described by others (for example, those employed by the CHAMP and GPS/MET groups[16,17]). The term $\Phi(\boldsymbol{x}, t)$ is a complex-valued phase envelope that modulates the received signal and is a function of time and position. Without considering unphysical receiver response, the geographic regions ($\boldsymbol{x}$) and times (t) where the real part of $\Phi(\boldsymbol{x}, t)$ is null should represent amplitude fading. The variations with respect to place and time in the complex phase angle of $\Phi(\boldsymbol{x}, t)$ are the physical cause of the changes in signal phase. This is complicated by the individual receiver response including loss of lock.

Velocity Augmentation

The spacecraft velocity, being roughly 10 times greater than velocities encountered in terrestrial applications, contributes to the scintillation effect. This is consistent with the cited references[16–18] describing phase screen and Able transform methodologies that explicitly model the observer (receiver) trajectory in LEO. For our purpose, we linearize $\Phi(\boldsymbol{x}, t)$ with respect to its spacial gradients and extract information about how velocity contributes to modulating $E(x, t)$. If the vehicle's velocity is large compared to the secular motions of the geophysical processes then we propose that essentially all the noise is a result of the motion of the spacecraft. We believe that to be the case because spread F and auroral structures in the ionosphere are persistent for several tens of minutes, whereas an LEO vehicle will transit these structures in a few seconds. Therefore, consider a velocity dependence resulting from the spacecraft velocity and spatial gradients in the envelope:

$$\Phi(\boldsymbol{x}, t) \approx \Phi(\boldsymbol{x}) + \int_0^t \boldsymbol{\nabla}\Phi(\boldsymbol{x}) \cdot \boldsymbol{V}\, \mathrm{d}t \tag{4}$$

We would like to identify the velocity perturbation with components parallel and perpendicular to the line of sight to the scintillated satellite. The dot product in the integral in Eq. (4) is then expressed as follow:

$$\begin{aligned} \frac{\mathrm{d}\Phi}{\mathrm{d}t} &\approx \boldsymbol{\nabla}\Phi(\boldsymbol{x}) \cdot \boldsymbol{V} \\ &= \nabla_\parallel \Phi(\boldsymbol{x}) V_\parallel + \nabla_\perp \Phi(\boldsymbol{x}) V_\perp \\ &= \nabla_\parallel \Phi(\boldsymbol{x}) V \cos\alpha + \nabla_\perp \Phi(\boldsymbol{x}) V \sin\alpha \end{aligned} \tag{5}$$

We argue that velocity-directed components of the gradient are negligible because the accumulation of paths that are contributing to the first-order variation is, in that case, nearly parallel to the line of sight. Certainly, parallel components of velocity contribute to Doppler shift but the receiver is already adapted to measure this for the range-rate observation. Neglecting the parallel component and substitution into Eq. (3) allows us to see how variations in the radiation electric field are modulated by the velocity and the phase envelope:

$$\delta E(\boldsymbol{x}, t) = E_0 e^{-i\omega t} \int_0^t \nabla_\perp \Phi(\boldsymbol{x}) V \sin\alpha\, \mathrm{d}t \tag{6}$$

Equation (6) suggests that we test the theory by examining distributions of scintillated signal relative to the angle that the line of sight makes with the spacecraft velocity vector, which we here identify as α with $\alpha = 0$ denoting forward direction.

Speculation About Faraday Rotation

Because the ionospheric plasma is magnetized, Faraday rotation, a preferred phase advance of the right-hand circularly polarized component of the electric field in a magnetized plasma, is a candidate for contributing to L-band scintillation. Klobuchar seems to report that the circular polarization of GPS signals protects against Faraday rotation.[6] We think the comment is intended to explain the practical benefit of circular polarization in receiving signals from an arbitrarily oriented antenna. There is no physical basis for any assertion that circular polarization implies that Faraday rotation is not a problem for GPS. It still represents a phase advance of the electric field. Rather, an analysis of the plasma dispersion relation shows that the high frequency of the L band compared to any conceivable cyclotron frequencies in the ionosphere effectively protects against first-order effects from Faraday rotation. Contributions to range-rate noise from any rapid modulation of a Faraday rotated electric field vector resulting in scintillation are not ruled out. This might manifest as enhanced noise for lines of sight parallel to the local magnetic field.

Velocity Angle Distribution

Identifying a null hypothesis that the signals are randomly distributed with respect to spacecraft velocity, the distribution of events with respect to angle from the velocity vector must then be proportional to $\sin\alpha$ because the solid angle available to intercept random lines of sight scales according to this factor. On the other hand, if signal events are proportional to the perpendicular component of velocity in accordance our with theory, then distribution must be further scaled by another factor of $\sin\alpha$ because $V \sin\alpha$ is the component of velocity perpendicular to the line of sight as seen in Eq. (6).

To test this, we accumulate statistics on the line of sight of scintillation events ($\sigma > 2$) compared to contemporaneous unscintillated measurements ($\sigma < 2$). These data were prepared by calculating the angle between the GPS satellite line of sight and the spacecraft velocity vector. Nominally, four satellites are tracked simultaneously. Distributions of angles are divided into two sets based on noise level. On STS 99, for example, we found 10,308 scintillation events characterized by noisy delta range ($\sigma > 2$). In this set we also found 25,266 satellite tracking intervals that exhibited just nominal signal level. Figure 4 presents the results. These histograms are normalized to unit integral with respect to angle. Normalized distributions of $\sin\alpha$ and $\sin^2\alpha$ are presented for reference. The units in Fig. 4 are reciprocal radians so that the integral with respect to radian angle will be dimensionless and, in this case, of unit magnitude.

We assert that scintillated events follow a $\sin^2\alpha$ distribution consistent with our theory whereas the "random" lines of sight conform closely to $\sin\alpha$, although we have not ruled out other possible selective factors such as latency in acquiring lock on satellites in the forward direction, for example. The same analysis for STS 88 supports the theory. The same analysis for the two other missions studied have less statistical confidence but do not contradict the results.

We are aware that the satellite selection algorithm for the GPS receiver is not strictly random. The receiver attempts to track four satellites with an optimal geometry. This puts an emphasis on selection of one high-elevation satellite and three other low-elevation satellites. We are not able to rule out an accidental clustering of scintillation according to a $\sin^2\alpha$ distribution, but we would not understand how to reconcile this with the $\sin\alpha$ of the nonscintillated satellite tracks. We would expect that these latter events would be depleted near 90 deg if we were accidentally selecting high-elevation satellites that were also scintillated. We should also point out that the selection logic permits satellites to track over significant arcs of the sky so that a high-elevation satellite eventually becomes 9 low-elevation one.

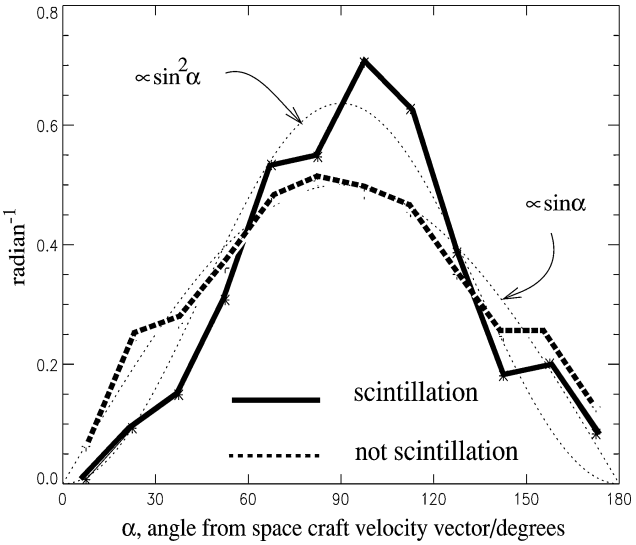

Fig. 4 STS 99 data: distribution of line of sight to GPS satellite vectors and local spacecraft velocity vector. Nonscintillated events should scale according to $\sin\alpha$, whereas the scintillated signals should distribute according to $\sin^2\alpha$. All series shown are normalized to unit integral with respect to α.

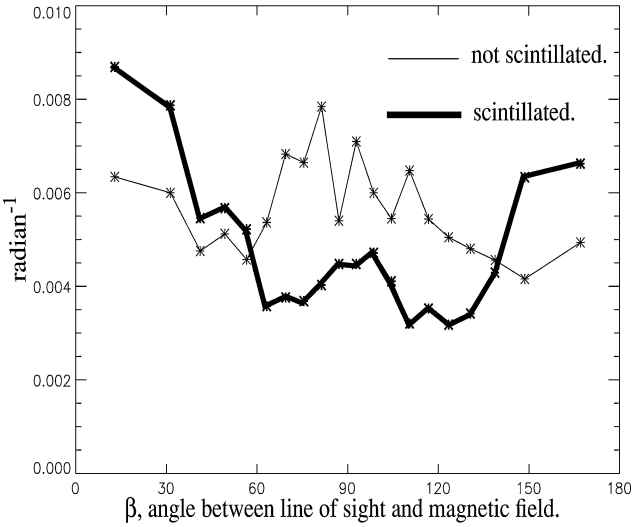

Fig. 5 Distribution of angles between satellite line of sight and geomagnetic field at location of spacecraft for the equatorial scintillation events from STS 88. Histogram bins are scaled according to equally spaced increments of $\cos^{-1}\beta$ compensating for $\sin\beta$ distribution of solid angle.

Magnetic Field

Plasma instabilities contributing to the spread F anomaly are restricted in motion to corotating flux tubes that are oriented along geomagnetic meridians. The importance of the magnetic field to mobility of ions and our suggestion that transient Faraday rotation contributes to scintillation encourages us to consider examining event distribution with respect to the angle of the line of sight using the same kind of analysis we performed for the velocity. Figure 5 represents our effort in this regard. Here, we have accumulated a histogram of the number of events in bins of angle of the line of sight from the geomagnetic field at the location of the spacecraft. As we mentioned previously, solid angle measures of random distributions are weighed toward perpendicular as a result of the increase in available solid angle as the perpendicular direction is approached. To compensate for this in Fig. 5 we have weighted the histogram bins so that the width of bins is proportional to the arc-cosine of the solid angle. The histograms are also normalized to unit integral with respect to angle.

There were 3635 scintillated events of 12,889 total events with dip-angle magnitude less than 45 deg. STS 99 and the other missions are similar. Although there is some tendency toward elevated levels at 0 and 180 deg, they are not supported statistically and we have not ruled out other coincidental reasons for that effect. We therefore report a null result for substantial clustering of the events with respect to angle between the magnetic field and line of sight to GPS satellites. It may be that the lines of sight directed along the magnetic field are intercepting more disordered regions of plasma as a result of the meridionally oriented instabilities. We would simply like to provoke further discussion and investigation in this area.

Conclusions

The essential physics of radiation through the ionosphere predicts that the medium will not attenuate at L-band frequencies. Scintillation occurs because there exist multiple available paths of propagation that are geometrically far apart and rapidly varying. Thus, amplitude fading and phase scintillation are not necessarily distinct physical phenomena but may reflect individual idiosyncratic receiver responses to the same interference envelope.

The GPS receiver selected for use on the space shuttle is subject to a spacecraft velocity augmented modulation of the interference envelope affecting range-rate observables. The interference occurs in the geographic regions and at solar hour angles consistent with previously identified ionospheric instabilities that cause scintillation.

The incidence of observed scintillation is highly variable. Equatorial events occur at night and cluster to within 20–30° of the magnetic equator corresponding to a dip-angle boundary between + or −45 deg, except for a few excursions outside that zone in the south-central equatorial Atlantic Ocean. The equatorial zone that we identify coincides with the location of ionospheric plasma instabilities identified with equatorial spread F. Solar-hour-angle occurrence is consistent with that conclusion although we see it occurring at later hours in the night than most of the literature. Polar events correspond to the auroral regions and exhibit known asymmetries consistent with the polar auroral oval systems.

The scintillation we observe in the MAGR/S is apparently augmented by the high velocity of the spacecraft because events are preferentially distributed at right angles to spacecraft motion in accordance with a theory we advance holding that the component of spacecraft motion perpendicular to the line of sight contributes to the interference. This appears to be the case at least for the MAGR/S receiver we are studying. If these observations are repeatable and the theory is further substantiated, we would like to offer it as a selective factor in weighting measurements for future space-rated receivers. The angle between the velocity vector and the line of sight to the GPS could be used to increase formal measurement uncertainty when the angle is close to perpendicular. We propose that this can mitigate high error in associated velocities.

Although the velocity noise resulting from scintillation exceeds normal space shuttle operational tolerances, the result of our theoretical analysis causes us to believe the noise is not a threat to safety. This is because the critical function of the receiver is only needed after the vehicle has deorbited and is approaching a landing site where velocity is close to that of the original terrestrial application that the receiver was designed for. The velocity noise we report here represents a deficiency in the receiver for use in orbit operations but the receiver is not formally required for that use. The situation does represent a close call because the noise was not anticipated and thus we regard the scintillation as a technical risk. Although formal requirements of the program have been met, no effort was ever engaged to improve or exceed existing requirements. We think these kinds of risks and the lost opportunity to improve productivity and safety need to be considered when using so-called off-the-shelf technologies.[8]

The observations support widespread geographical distribution of scintillation in equatorial regions consistent with ground-based and global modeling of the phenomenon. Seasonal variability may also be present but a satisfactory explanation of the variability from mission to mission should await more careful analysis, comparing these observations with the existing research models of the phenomenon. We submit that the known selective factors such as magnetic activity are modified, even as Aarons[3] points out, by seasonal or synoptic scale variability in the neutral atmosphere abundance and neutral winds such as these are the parameters that are the least well understood.

Acknowledgment

These materials are sponsored by NASA under Contract NAS9-20000.

References

[1]Goodman, J. L., and Kramer, L., "Scintillation Effects on Space Shuttle GPS Data," *Proceedings of the National Technical Meeting*, Inst. of Navigation, Alexandria, VA, Jan. 2001.

[2]Goodman, J. L., "Parallel Processing GPS Augments TACAN in the Space Shuttle," *GPS World*, Vol. 15, No. 10, 2002, pp. 20–26.

[3]Aarons, J., "The Longitudinal Morphology of Equatorial F-Layer Irregularities Relevant to Their Occurrence," *Space Science Reviews*, Vol. 63, No. 1–4, 1993, pp. 209–243.

[4]Sobral, J. H. A., Abdu, M. A., Takahashi, H., Taylor, M. J., de Paula, E. R., Zamlutti, C. J., de Aquino, M. G., and Borba, G. L., "Ionospheric Plasma Bubble Climatology over Brazil Based on 22 Years (1977–1998) of 630 nm Airglow Observations," *Journal of Atmospheric and Solar-Terrestrial Physics*, Vol. 64, No. 12–14, 2002, pp. 1517–1524.

[5]Kelley, M. C., *The Earth's Ionosphere: Plasma Physics and Electrodynamics*, Academic Press, San Diego, CA, 1989.

[6]Klobuchar, J. A., "Ionospheric Effects on GPS," *Global Positioning System: Theory and Applications*, edited by B. W. Parkinson, J. J. Spilker Jr., P. Axelrod, P. Enge, and P. Zarchan, AIAA, Reston, VA, 1996, pp. 485–515.

[7]Pi, X., Mannucci, A. J., Lindqwister, U. J., and Ho, C. M., "Monitoring of Global Ionospheric Irregularities Using the Worldwide GPS Network," *Geophysical Research Letters*, Vol. 24, No. 18, 1997, pp. 2283–2286.

[8]Goodman, J. L., "The Space Shuttle and GPS—A Safety-Critical Navigation Upgrade," *Proceedings of the 2nd International Conference on COTS-Based Software Systems*, Vol. 2580, Springer-Verlag Lecture Notes in Computer Science, 2003, pp. 92–100.

[9]Bishop, G., Basu, S., Holland, E., and Secan, J., "Impacts of Ionospheric Fading on GPS Navigation Integrity," *Proceedings of ION GPS-94*, Inst. of Navigation, Alexandria, VA, 1994, pp. 577–585.

[10]Doherty, P. H., Delay, S. H., Valledares, C. E., and Klobuchar, J. A., "Ionospheric Scintillation Effects in the Equatorial and Auroral Regions," *Proceedings of ION GPS-2000*, Inst. of Navigation, Alexandria, VA, 2000, pp. 662–671.

[11]Anderson, D. N., "A Theoretical Study of the Ionospheric F Region Equatorial Anomaly-II. Results in the American and Asian Sectors," *Planetary and Space Science*, Vol. 21, No. 3, 1973, pp. 421–442.

[12]Basu, S., and Valladares, C., "Global Aspects of Plasma Structures," *Journal of Atmospheric and Solar-Terrestrial Physics*, Vol. 61, No. 1–2, 1999, pp. 127–139.

[13]Whalen, J. A., "Equatorial Bubbles Observed at the North and South Anomaly Crests: Dependence on Season, Local Time and Dip Latitude," *Radio Science*, Vol. 32, No. 4, 1997, pp. 1559–1566.

[14]Feynman, R. P., *QED: The Strange Theory of Light and Matter*, Princeton Univ. Press, Princeton, NJ, 1985.

[15]Landau, L. D., and Lifshitz, E. M., *The Classical Theory of Fields*, Pergamon, Oxford, 1975.

[16]Sokolovskiy, S. V., "Modeling and Inverting Radio Occultation Signals in the Moist Troposphere," *Radio Science*, Vol. 36, No. 3, 2001, pp. 441–458.

[17]Beyerle, G., Hocke, K., Wickert, J., Schmidt, T., Marquardt, C., and Reigber, C., "GPS Radio Occultations with CHAMP: A Radio Holographic Analysis of GPS Signal Propagation in the Troposphere and Surface Reflections," *Journal of Geophysical Research*, Vol. 107, No. D24, 4802, 2002, pp. ACL 27-1–27-14.

[18]Hajj, G. A., and Romans, L. J., "Ionospheric Electron Density Profiles Obtained with the Global Positioning System: Results from GPS/MET Experiment," *Radio Science*, Vol. 33, No. 1, 1998, pp. 175–190.

[19]Swanson, D. G., *Plasma Waves*, Academic Press, Boston, 1989.

[20]Klobuchar, J. A., "Real-Time Ionospheric Science: The New Reality," *Radio Science*, Vol. 32, No. 5, 1997, pp. 1943–1952.

N. Gatsonis
Associate Editor